Nanostructures

DOI: 10.1002/ange.200501282

PbTe Nanorods by Sonoelectrochemistry**

*Xiaofeng Qiu, Yongbing Lou, Anna C. S. Samia, Anando Devadoss, James D. Burgess, Smita Dayal, and Clemens Burda**

Size, shape, and compositional control are at the heart of nanochemistry.[1] Herein, we present a novel method that allows control over all three variables in a simple one-step, wet-chemical procedure. One-dimensional (1D) nanomaterials are of great interest for the construction of high-performance thermoelectric (TE) devices. Theoretical calculations indicate that improvement in TE efficiency can be achieved as the diameter of the 1D structures approaches a few nanometers.[2,3] To date, the most successful synthesis of 1D TE materials has been achieved by electrodeposition within alumina templates. A series of Bi_2Te_3,[4,5] $Bi_{2-x}Sb_xTe_3$,[6] $Bi_2Te_{3-y}Se_y$,[7] and $Bi_{1-x}Sb_x$[8,9] nanowires were prepared by using the template-based method. The advantages of the electrodeposition method include high efficiency, ease of control over composition, highly crystalline products, and room-temperature reaction conditions. However, the diameters of the nanowires synthesized by the template method are well above 10 nm. To get into the sub-10-nm regime, one needs to obtain templates with very narrow channel diameters, which is currently the limiting factor of this technique.

However, advances in combining sonochemistry and electrochemistry have provided a new strategy for the synthesis of nanomaterials.[10–13] The synthesis of quite sophisticated 1D nanomaterials has recently been demonstrated[14] to be possible through careful control of the electrochemistry, sonochemistry, and initial composition of the precursor solutions. As observed, the advantage of the sonoelectrochemical method is that it achieves 1D control without any template, thereby practically overcoming the limitation of generating nanorods with diameters below 10 nm. This diameter is the size regime in which TE properties become enhanced and a controlled synthesis can produce technologically relevant nanomaterials. Herein, we report the first synthesis of monodispersed PbTe nanorods that are sub-10 nm in diameter through a sonoelectrochemical technique.

[*] X. Qiu, Y. Lou, Dr. A. C. S. Samia, S. Dayal, Prof. C. Burda
Center for Chemical Dynamics and Nanomaterials Research
Department of Chemistry
Case Western Reserve University
10900 Euclid Avenue, Cleveland, OH 44106 (USA)
Fax: (+1) 216-368-3006
E-mail: burda@case.edu
A. Devadoss, Prof. J. D. Burgess
Department of Chemistry
Case Western Reserve University
10900 Euclid Avenue, Cleveland, OH 44106 (USA)

[**] C.B. acknowledges support from NSF (CHE-0239688), ACS-PRF (39881-G5M), and the Ohio Board of Regents.

Furthermore, we present the effect of changing the concentration of the coordinating ligand on the resulting composition of the synthesized nanomaterials. Changing the metal/ligand ratio enabled us to tune the composition of the product from pure Te to pure PbTe nanorods.

Lead telluride is the material of choice because of its great potential in high-performance TE devices.[15] Furthermore, it allows the mechanisms that lead to control over the resulting nanorod size and composition to be studied. Basically, the synthesis of PbTe nanorods consists of two steps: First, the electrodeposition of PbTe on the surface of the Ti sonication horn, and second, the dispersion of the PbTe nuclei into solution by pulsed sonication. Control over the electrodeposition process is crucial in obtaining pure and highly crystalline PbTe nanoparticles. Interestingly, we found that the Pb^{2+}/nitrilotriacetic acid (NTA) ratio plays a key role in the synthesis of PbTe nanorods. In contrast to previous studies on the electrodeposition of bulk PbTe,[16] we used a stoichiometric reactant ratio in the synthesis of the nanorods. The introduction of NTA helps to prevent the precipitation of Pb^{2+} ions as $Pb(OH)_2$. Furthermore, electrochemical studies show that NTA acts as more than a coordinating capping agent: it actually determines the final products of the process. The pH value of the solution was monitored during the electrodeposition, and TeO_2 was shown to be sufficiently soluble at $pH < 2$ or $pH > 7$.[16] However, the solubility of NTA was too poor at low pH values to keep the Pb^{2+} ions coordinated and in solution. Therefore, the solution was kept at approximately pH 8 under our experimental conditions, as TeO_2 is dissolved as TeO_3^{2-} ions at this pH value. The overall PbTe reaction equation [Eq. (1)] is (the NTA ligand is omitted for clarity):

$$Pb^{2+} + TeO_3^{2-} + 3\,H_2O + 6\,e^- \rightarrow PbTe + 6\,OH^- \quad (1)$$

Figure 1 shows the cyclic voltammograms of solutions with different NTA concentrations. In this figure, peaks 1, 1′, and 1″ correspond to the reduction of TeO_3^{2-} to Te^{2-} while peaks 2, 2′, and 2″ correspond to the reduction of TeO_3^{2-} to Te^0.[16,17] The potential shifts show that the electrodeposition of PbTe is highly sensitive to the ratio between Pb^{2+} and NTA.

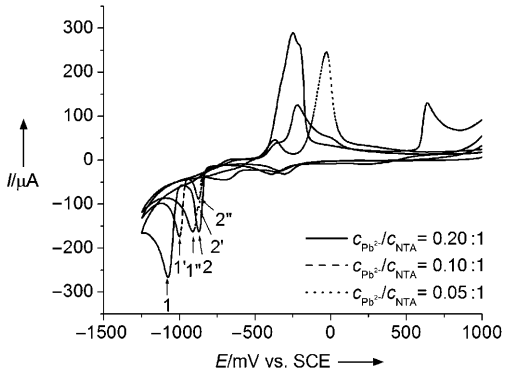

Figure 1. Cyclic voltammogram of the precursor solutions with $c_{Pb^{2+}}/c_{NTA}$ ratios changing from 0.20:1 (solid) to 0.10:1 (dash) then to 0.05:1 (dot). The concentrations of Pb^{2+} and TeO_3^{2-} ions were fixed at 10 mM in all measurements. SCE = saturated calomel electrode.

At ratios of Pb^{2+}/NTA higher than approximately 0.16:1, the formation of PbTe can be achieved at potentials lower than −1.0 V and only the oxidation peak of PbTe at −0.245 V is observed in the reverse scan. By decreasing the Pb^{2+}/NTA ratio to as low as 0.05:1, peaks 1″ and 2″ almost overlap and the predominant species produced is Te^0, which is proved by the predominant oxidation of Te at −0.029 V during the reverse scan. The precipitation of both PbTe and Te^0 are observed in the intermediate cases in which the Pb^{2+}/NTA ratios are between 0.20:1 and 0.05:1, even when the potential is kept below −1.0 V. Both the oxidation peaks of PbTe at −0.225 V and Te at −0.024 V can be clearly observed in the reverse scan. This tuning of the product outcome was also confirmed by powder X-ray diffraction (XRD) measurements of the isolated nanomaterials. Overall, this observation shows that the Pb^{2+}/NTA ratio controls the nature and concentration of Pb^{2+} ions in solution, which then in turn influences the formation of PbTe.[18] Basically, the PbTe formation predominates when the Pb^{2+}/NTA ratio is high, even at very low concentrations of Te^{2-} ions. However, if the Pb^{2+}/NTA ratio is too low, the thermodynamic solubility constant K_{sp} limits the precipitation of PbTe, which only occurs at relatively high concentrations of Te^{2-} ions. We observed similar phenomena for the synthesis of other semiconductor nanocrystals. These results show that the ratio of metal ion/ligand concentration can be the controlling factor in the redox chemistry involved in the synthesis of semiconductor nanomaterials.

Figure 2 shows the powder XRD pattern of nanorods produced under different Pb^{2+}/NTA ratios. The XRD patterns show that the product exhibits a purely face-centered cubic (fcc) PbTe system ($a = 6.464$ Å; JCPDS card: 78-1905) at a high Pb^{2+}/NTA ratio (a), whereas the product is a purely

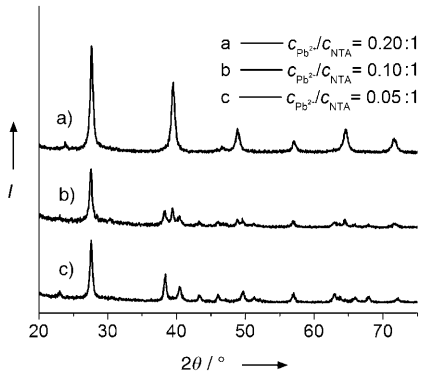

Figure 2. The powder XRD pattern of nanorods synthesized at different Pb^{2+}/NTA ratios. a) Pure PbTe, b) mixture of PbTe and Te, and c) pure Te.

hexagonal tellurium system ($a = 4.457$, $c = 5.927$ Å; JCPDS card: 36-1452) at low Pb^{2+}/NTA ratios of ≤ 0.05:1 (c). The XRD patterns for the products made at intermediate concentration ratios indicate a mixture of PbTe and Te powder. The cyclic voltammetry (CV) and XRD studies together show that the composition of the sample can be controlled by the initial Pb^{2+}/NTA ratio.

Modulation of the morphology is achieved by controlling the current intensity, reagent concentration, reaction time, and ultrasound intensity, as well as the ultrasound pulse on/off ratio. The morphology and crystallinity of the PbTe nanoparticles can be controlled precisely by using the correct sonoelectrochemical conditions.

A transmission electron microscopy (TEM) image of the PbTe nanorods shows a highly uniform nanorod morphology (Figure 3a), in which the nanorods have an average diameter of 7 nm and an aspect ratio of 7. It was found that the reaction time greatly affects the size of the PbTe nanorods and increasing the reaction time yielded larger nanorods with larger aspect ratios. Figure 3c shows the morphology of a PbTe nanorod after reaction for 45 minutes. The resulting nanorod has a diameter of 11.4 nm and a length of 104 nm. Figure 3d shows the nanorod obtained after 1.5 hours, which

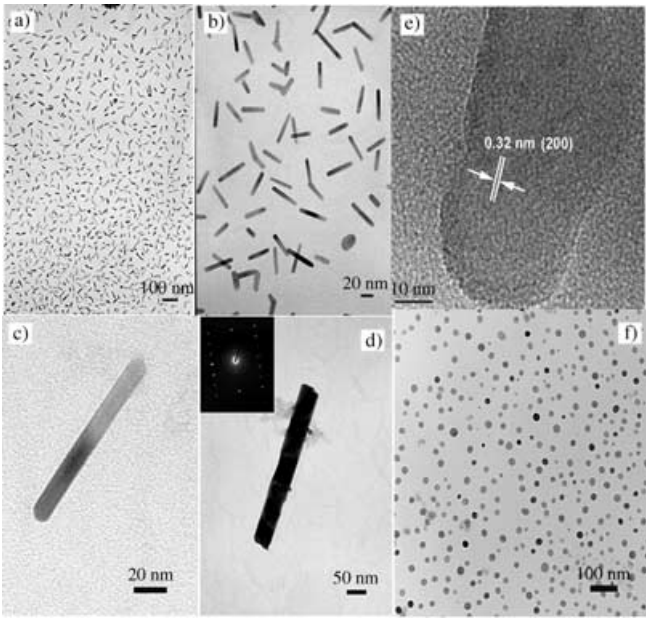

Figure 3. a) TEM image of PbTe nanorods prepared by sonoelectrochemistry at room temperature for 30 minutes. b) Enlarged TEM image of PbTe nanorods prepared under identical conditions. c) TEM image of a nanorod obtained after 45 minutes of reaction. d) TEM image of a nanorod obtained after 1.5 hours of reaction; the inserted selected-area electron-diffraction pattern indicates the single-crystal nature of the shown nanorod. e) HRTEM image of PbTe, a nanorod indicating the (200) lattice plane spacing. f) Spherical PbTe nanoparticles synthesized under a low concentration of Pb^{2+} ions (2 mM).

has a diameter of 43 nm and a length of 370 nm. A high-resolution TEM (HRTEM) study (Figure 3e) shows that the PbTe nanorods are highly crystalline and that the d spacing is 0.32 nm, which indexes to the $d(200)$ planes of the fcc PbTe lattice. This value corresponds exactly to the strongest peak observed in the XRD pattern (Figure 2a). Therefore, the direction of the nanorod growth is perpendicular to the x axis and is along the [001] plane. Figure 3f shows PbTe nanoparticles synthesized under a very low concentration of Pb^{2+} ions (2 mM), and only spherical particles are observed. Increasing the concentration of Pb^{2+} ions causes the spheres to grow and rod-shaped morphologies to be yielded. Such rod growth is likely to occur through Ostwald ripening under the ultrasound cavitation process. Similar growth mechanisms were reported in the thermal synthesis of CdTe nanowires and Ag nanorods.[19,20]

As the XRD results show, the prepared PbTe nanorods exhibit a cubic lattice structure. The crystalline symmetry of the material also affects the ZT value of the TE materials. Cubic space groups yield maximum degeneracy N_v of the band extrema near the Femi level. The ZT value, which is of merit itself, is proportional to the N_v value.[21] Thus, a further enhancement of the TE power can be reached with cubic PbTe nanorods.

In conclusion, we have successfully achieved the synthesis of PbTe nanorods with a diameter in the sub-10-nm regime that are highly uniform, single-crystalline, and pure through a novel sonoelectrochemical method under ambient conditions. The ratio of metal ion/ligand was used to control the purity of the PbTe nanostructures. These very thin and cubic PbTe nanorods are promising building units for future TE devices. Currently, the sonoelectrochemical synthesis of other nanomaterials is being studied to show the usefulness of this procedure for a broad range of synthetic applications.

Experimental Section

The room-temperature synthesis of the PbTe nanorods is based on constant-current electrodeposition accompanied by applied ultrasonic pulses in an aqueous solution that contains lead nitrate (Aldrich, 99.99%), NTA (Aldrich, 99+%), and TeO_2 (Aldrich, 99+%). A VCX-500 ultrasonic processor from Sonics and Materials Inc. (Ti horn, 0.5 inch in diameter, 20 kHz) worked as the ultrasound source and a Harrison 6102 A DC power supply acted as the current source. The solution was sonicated in the presence of a constant current for 0.5–2 h, and a sonication pulse on/off ratio varying from 1:1 to 1:10 was explored for the nanorod synthesis. Highly crystallized and monodispersed PbTe nanorods were produced with current densities of 10 mA cm^{-2}, ultrasound intensities of approximately 25–45%, and a reaction time of 30 min. After the reaction, the resulting brown–black solution was purified by centrifugation, and the precipitate was washed with distilled water and ethanol and then air dried before analysis.

CV measurements were carried out on a BAS CV 50W with a Pt-disc working electrode, Pt-wire counter electrode, and an SCE reference electrode, and the scan rate was 100 mV s^{-1}. The phase purity of products was characterized by a Scintag X-1 Advanced X-ray diffractometer (XRD, 2.4° min^{-1}, $Cu_{K\alpha}$ radiation). The morphology of the PbTe nanorods was analyzed with a transmission electron microscope, JEOL 1200CX (TEM, accelerating voltage: 80 kV). The HRTEM images were obtained on a FEI Tecnai F30 electron microscope by applying an accelerating voltage of 300 kV.

Received: April 12, 2005
Revised: June 4, 2005
Published online: August 5, 2005

Keywords: electrochemistry · nanorods · PbTe · sonochemistry

[1] C. Burda, X. Chen, R. Narayanan, M. A. El-Sayed, *Chem. Rev.* **2005**, *105*, 1025–1102.
[2] L. D. Hicks, M. S. Dresselhaus, *Phys. Rev. B* **1993**, *47*, 16631–16634.
[3] Y. M. Lin, M. S. Dresselhaus, *Phys. Rev. B* **2003**, *68*, 75304–75314.
[4] S. A. Sapp, B. B. Lakshmi, C. R. Martin, *Adv. Mater.* **1999**, *11*, 402–404.
[5] A. L. Prieto, M. S. Sander, M. S. Martin-Gonzalez, R. Gronsky, T. Sands, A. M. Stacy, *J. Am. Chem. Soc.* **2001**, *123*, 7160–7161.
[6] M. Martin-Gonzalez, A. L. Prieto, R. Gronsky, T. Sands, A. M. Stacy, *Adv. Mater.* **2003**, *15*, 1003–1006.
[7] M. Martin-Gonzalez, G. J. Snyder, A. L. Prieto, R. Gronsky, T. Sands, A. M. Stacy, *Nano Lett.* **2003**, *3*, 973–977.
[8] A. L. Prieto, M. Martin-Gonzalez, J. Keyani, R. Gronsky, T. Sands, A. M. Stacy, *J. Am. Chem. Soc.* **2003**, *125*, 2388–2389.
[9] M. Martin-Gonzalez, A. L. Prieto, M. S. Knox, R. Gronsky, T. Sands, A. M. Stacy, *Chem. Mater.* **2003**, *15*, 1676–1681.
[10] J. Reisse, T. Caulier, C. Deckerkheer, O. Fabre, J. Vandercammen, J. L. Delplancke, R. Winand, *Ultrason. Sonochem.* **1996**, *3*, S147–S151.
[11] J. J. Zhu, S. T. Aruna, Y. Koltypin, A. Gedanken, *Chem. Mater.* **2000**, *12*, 143–147.
[12] Y. Mastai, R. Polsky, Y. Koltypin, A. Gedanken, G. Hodes, *J. Am. Chem. Soc.* **1999**, *121*, 10047–10052.
[13] Y. Mastai, M. Homyonfer, A. Gedanken, G. Hodes, *Adv. Mater.* **1999**, *11*, 1010–1013.
[14] X. F. Qiu, C. Burda, R. L. Fu, L. Pu, H. Y. Chen, J. J. Zhu, *J. Am. Chem. Soc.* **2004**, *126*, 16276–16277.
[15] T. C. Harman, P. J. Taylor, M. P. Walsh, B. E. LaForge, *Science* **2002**, *297*, 2229–2232.
[16] H. Saloniemi, M. Kemell, M. Ritala, M. Leskela, *J. Electroanal. Chem.* **2000**, *482*, 139–148.
[17] H. Saloniemi, T. Kanniainen, M. Ritala, M. Leskela, *Thin Solid Films* **1998**, *326*, 78–82.
[18] G. Riveros, D. Lincot, J. F. Guillemoles, R. Henriquez, R. Schrebler, R. Cordova, H. Gomez, *J. Electroanal. Chem.* **2003**, *558*, 9–17.
[19] Z. Tang, N. A. Kotov, M. Giersig, *Science* **2002**, *297*, 237–240.
[20] B. A. Korgel, D. Fitzmaurice, *Adv. Mater.* **1998**, *10*, 661–665.
[21] F. J. DiSalvo, *Science* **1999**, *285*, 703–706.

